

## Article

# Bioaccumulation and Potential Risk Assessment of Heavy Metals in Tropical Bamboo Plantations of *Dendrocalamus brandisii* under Two Cultivation Patterns in Yunnan, China

Qian Cheng <sup>1,2,†</sup> , Peitong Dou <sup>1,†</sup> , Changyan Bao <sup>1,\*</sup> , Zhiming Zhang <sup>1</sup>, Yurong Cao <sup>1</sup> and Hanqi Yang <sup>1,3,\*</sup> 

<sup>1</sup> Institute of Highland Forest Science, Chinese Academy of Forestry, Bailongsi, Panlong District, Kunming 650233, China; cq08042@caf.ac.cn (Q.C.); fordpt15@caf.ac.cn (P.D.); zhangzhiming@caf.ac.cn (Z.Z.); caoyurong@caf.ac.cn (Y.C.)

<sup>2</sup> College of Landscape Architecture, Nanjing Forestry University, Nanjing 210037, China

<sup>3</sup> Key Laboratory of Breeding and Utilization of Resource Insects, National Forestry and Grassland Administration, Kunming 650233, China

\* Correspondence: baochangyan@caf.ac.cn (C.B.); yanghanqikm@caf.ac.cn (H.Y.)

† These authors contributed equally to this work.

**Abstract:** Heavy metal (HM) pollution nowadays is a hot issue concerning global ecological and food safety. As one of the most important woody bamboos for edible shoots in Southeast Asia and southwest China, *Dendrocalamus brandisii* usually occurs in red soil with a high HM geological background. However, the bioaccumulation process and possible risks of HMs in their cultivation area remain unclear. In this study, a comprehensive risk assessment of HM pollution was conducted in the main cultivation area of *D. brandisii* under two cultivation patterns in Yunnan, China. The results revealed that moderate to heavy HM pollution existed in the soil of the study area, while bamboo shoots displayed either no pollution or weak contamination. The “large-area intensive afforestation” cultivation pattern can better control HM pollution in soil and shoots than the “small-scale farmer management” pattern. Strong and complex correlations among HMs were unveiled in both soil and shoot samples. The Cr content of 39% of the shoot samples exceeded China’s national standards. Cu and Zn were the two most easily accumulated HMs in shoots, with BCF of 0.1235 and 0.1101, respectively. Bioaccumulations of As and Cd were positively correlated with their concentrations in soil. Furthermore, the positive matrix factorization model (PMF) identified three main sources of soil HMs, i.e., Pb and Zn from traffic emissions accounting for 30%; Ni, Mn, and Cr from pedogenic parent material making up 35.4%; and As from mining and metallurgical activities accounting for 34.6%. Monte Carlo simulations suggested the probability of total noncarcinogenic risk for children from bamboo shoots was 24.82% and that As in the soil was the primary element of health risk to children (HQ<sub>c</sub> = 13.94%). These findings emphasize the urgent need to control and mitigate HM pollution from the identified sources and may contribute to the sustainable cultivation of *D. brandisii* and food safety in Yunnan and similar tropical areas with high HM contents.

**Keywords:** heavy metals; *Dendrocalamus brandisii*; source apportionment; positive matrix factorization model; Monte Carlo simulation



**Citation:** Cheng, Q.; Dou, P.; Bao, C.; Zhang, Z.; Cao, Y.; Yang, H. Bioaccumulation and Potential Risk Assessment of Heavy Metals in Tropical Bamboo Plantations of *Dendrocalamus brandisii* under Two Cultivation Patterns in Yunnan, China. *Forests* **2024**, *15*, 41. <https://doi.org/10.3390/f15010041>

Received: 16 October 2023

Revised: 19 December 2023

Accepted: 21 December 2023

Published: 23 December 2023



**Copyright:** © 2023 by the authors. Licensee MDPI, Basel, Switzerland. This article is an open access article distributed under the terms and conditions of the Creative Commons Attribution (CC BY) license (<https://creativecommons.org/licenses/by/4.0/>).

## 1. Introduction

Heavy metal (HM) pollution is a current focal issue worldwide because of its detrimental impacts on the ecological environment and human health [1,2]. The bioaccumulation of HMs in the natural environment increases serious risks to ecosystems and raises concerns about food safety and human health [3,4]. Among the regions known for high background levels of HMs, Yunnan Province of China has gained particular attention [5–9] and faces potential risks in both human health and the natural environment due to the unique geological features and long history of mining [10]. Therefore, understanding the accumulation

and source of HM contamination in the soil of Yunnan is crucial for assessing the potential risks and implementing effective mitigation strategies.

So far, multiple detection and analysis methods have been developed for the assessment of environmental HM pollution. HMs in soil originate from natural lithospheric weathering and human activities [11,12] and can be detected using soil profile differentiation [13,14]. Meanwhile, the positive matrix factorization model (PMF), pollution indices ( $P_i$ ), edge analysis, geoaccumulation indices ( $I_{geo}$ ), enrichment factors (EF), and GeogDetector model [15–18], and chemical mass balance are commonly employed to quantify the sources, contributions, and pollution status of HM pollutants [19,20]. Taken together, these methods can provide a more accurate analysis of pollution characteristics and source identification associated with HMs.

More importantly, the probabilistic impact of environmental pollutants on human health has attracted increasing attention. Extensive studies have investigated the potential health risks posed by HM contaminants to exposed populations using health risk assessment models and put forward suggestions to mitigate the risks [21–23]. Among current health risk assessment models, Monte Carlo simulation has been widely adopted to implement probabilistic risk assessment due to its high credibility [24–26].

Bamboo shoot is a kind of delicious and highly nutritious vegetable and is popular among people in Asia, and China is the world's largest producer of bamboo shoots [27]. *Dendrocalamus brandisii* (Munro) Kurz, a large-scale tropical bamboo species 10–20 m in height and 10–18 cm in culm diameter, is of high economic value for its sweet and nutritious bamboo shoots. This species occurs in China, Myanmar, Laos, Vietnam, and Thailand and has been introduced into East and South China since 1995 [28,29]. Currently, the cultivation and management of *D. brandisii* in Yunnan can be classified into two main patterns: small-scale farmer management (SF) and large-area intensive afforestation (LA). In the SF mode, bamboo clumps are typically cultivated in small-scale areas near houses, villages, roads, water sources, or other limited spaces (often <1 ha). Practices such as fertilization are commonly employed in SF cultivation to obtain high yields. On the other hand, the LA pattern adopts intensive cultivation of bamboo clumps in the planned mountainous areas on a larger scale (often >10 ha). This pattern aims to mimic or closely resemble natural conditions, ensuring a balance between forestry production and the conservation of forest ecosystems, with an emphasis on close-to-nature management. The LA pattern involves as little human intervention as possible, resulting in a smaller impact on soil quality and HM content in the cultivated areas. At present, the SF pattern is the traditional and predominant cultivation approach of *D. brandisii* in Yunnan, while the LA pattern is less widely adopted due to its higher investment requirements compared to the SF mode. Due to the high economic value of *D. brandisii*, its cultivation area has been increasing yearly [28,30], and the main cultivation area in China is central and southern Yunnan, which is rich in mineral resources [31]. However, the potential impacts and risks of the HMs on bamboo shoots remain unstudied.

For the sustainable development of the bamboo planting industry and people's health, an integrative study on the potential health risks of HM exposure is urgently needed. In this study, a detailed investigation of HM pollution in the *D. brandisii* cultivation area was carried out to predict the spatial distribution and bioaccumulation of HMs. Our aims are to: (1) detect the pollution status and spatial distribution of HM contents in bamboo shoots and soils of bamboo stands under different cultivation patterns; (2) identify the source and contribution of HMs in the soils of bamboo stands; and (3) assess the ecological and health risks of bamboo shoots and soil. The results will not only reveal the effect of soil HMs on bamboo shoots in a region with a high HM geological background and similar areas but also develop countermeasures for the risk management and remediation of HM pollution in tropic bamboo cultivation.

## 2. Materials and Methods

### 2.1. Study Area

The study area is located in six counties in the main distribution area of *D. brandisii*, including Xinping, Shiping, Mojiang, Ning'er, Jinggu, and Pu'er (Figure 1). Their geographic scope is 22°42'–24°8' N and 100°50'–102°32' E. The soil of *D. brandisii* stands as sandy red soil with a pH range of 3.7–7.9. Rhizosphere soil and shoot samples of typical bamboo forests were collected in the region mentioned above.

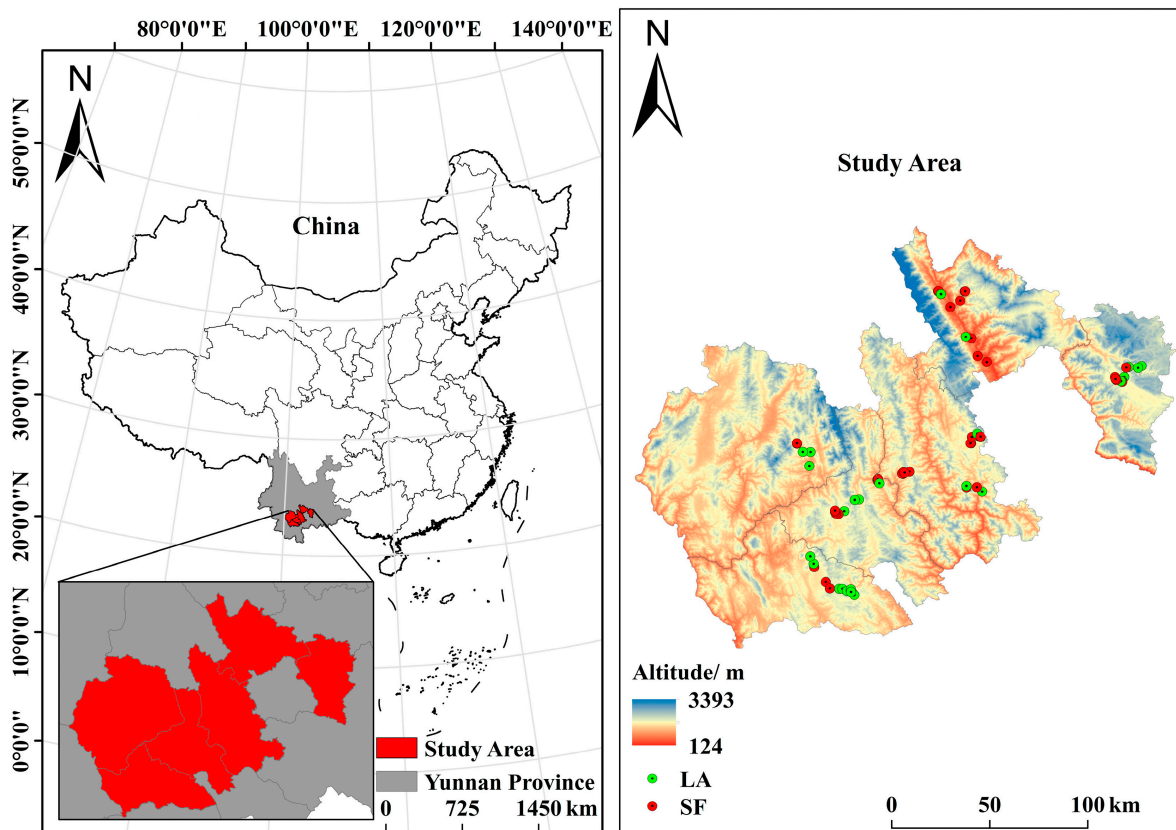


**Figure 1.** Location map of sampling points in the study area. LA, bamboo forests of the large-area intensive afforestation pattern; SF, bamboo forests of the small-scale farmer management pattern.

### 2.2. Sample Collection

A total of 148 samples from 74 quadrats, including 74 bamboo shoot samples and 74 soil samples, were collected from August 2021 to September 2022 (Figure 1). Among them, 34 quadrats were in the LA pattern, and 40 quadrats were in the SF pattern. During the bamboo shoot harvesting season, fresh bamboo shoot samples (ca. 1 kg) were collected and stored in liquid nitrogen and then immediately transported to the laboratory for subsequent analyses. Simultaneously, the subsurface rhizosphere soil (0–20 cm) around the rhizome was collected using the “S”-shaped uniform random method. Five soil samples collected at each quadrat were mixed, and the mass of the combined sample was 0.5 kg. In order to qualitatively analyze the sources of HMs, 15 soil samples were collected from five 60 cm-depth soil profiles, three profiles from the SF pattern (Profiles 1–3), and two profiles from the LA pattern (Profiles 4 and 5). The soil layers of the profile were categorized as layers A (0–20 cm), B (20–40 cm), and C (40–60 cm). All soil samples were air-dried at 25 °C and sieved with a 2 mm mesh, and then approximately 50 g of each sample was ground again and sieved through a 0.15 mm mesh. The final samples were placed in a polyethylene film-sealed bag with a label and stored for further analysis.

### 2.3. Chemical Analysis

Approximately 1 g of each bamboo shoot sample was transferred to a Teflon tube with an acid digestion mixture (5 mL HNO<sub>3</sub>, 2 mL H<sub>2</sub>O<sub>2</sub>) [16]. Approximately 0.5 g of each soil sample was digested in a Teflon digestion vessel with an acid digestion mixture (aqua regia 6 mL, HCL and HNO<sub>3</sub>, 3:1 v/v; 2 mL HF) [11]. The sealed samples were placed into the microwave digestion instrument. The digestion program was set as 5 min ramp to 130 °C for 120 min, then 5 min ramp to 180 °C for 60 min. Then, the acid solution in the digestion tank was evaporated, and the sample volume was adjusted to 50 mL with distilled water. Afterwards, the contents of eight key HMs, including As, Cr, Pb, Cd, Ni, Zn, Cu, and Mn, were determined via ICP-MS (Agilent Technologies 7700x, Bremen, Germany). The pH values of soil samples were determined at the soil/water ratio of 1:2.5. Each sample was measured three times.

### 2.4. Assessment of Pollution Indices

The coefficient of variation (CV) of soil and shoot samples was calculated according to Equation (1):

$$CV = \frac{\sigma}{\mu} \quad (1)$$

where  $\sigma$  was the standard deviation of HMs content and  $\mu$  was the average value.

To accurately evaluate the ecological risk of HM contamination in soil,  $P_i$ ,  $I_{geo}$ , and potential ecological risk index (RI) were conducted together in this study.  $P_i$  is calculated according to Equation (2):

$$P_i = \frac{C_i}{C_n} \quad (2)$$

where  $C_i$  (mg/kg) was the actual measured concentration of HMs in the soil sample;  $C_n$  was the reference standard concentration value of each metal element in the soil sample. The soil environmental quality standards of China (GB15618-2018) [32] were used as reference standards, and  $P_i$  was divided into five grades (Table S1).

The HM pollution status of soil was calculated according to Equation (3):

$$I_{geo} = \log_2 \left( \frac{C_n^i}{1.5B_n^i} \right) \quad (3)$$

where  $C_n^i$  was the concentration of examined HM  $i$  in the soil sample (mg/kg), and  $B_n^i$  was the background value of the HM  $i$  in the soil of Yunnan (mg/kg) [5].  $I_{geo}$  contamination was categorized into seven classes (Table S2).

The comprehensive potential ecological risk (RI) was calculated according to Equation (4):

$$RI = \sum_{i=1}^n E_r^i = \sum_{i=1}^n \left( T_r^i \times \frac{C_n^i}{B_n^i} \right) \quad (4)$$

where  $T_r^i$  was the toxicity coefficient for HM  $i$ ;  $C_s^i$  was the actual measured concentration of HMs; and  $C_B^i$  was the metal background value. According to Hakanson (1980), the toxicity coefficients for Cr, Mn, Ni, Cu, Zn, As, Cd, and Pb were set to 2, 1, 5, 5, 1, 10, 30, and 5, respectively [33]. Based on the values of  $E_r^i$  and RI, the classifications of pollution levels are presented in Table S3.

Bioconcentration factor (BCF) was used to identify the accumulation and transfer ability of HMs from soil to the bamboo shoots and was calculated according to Equation (5):

$$BCF = \frac{C_b}{C_s} \quad (5)$$

where  $C_b$  was the concentration of HMs in the bamboo shoot samples;  $C_s$  was the soil HM concentration in the corresponding rhizosphere soil samples.

### 2.5. PMF Model

The PMF model was a receptor model for pollutant source analysis [34] and was calculated according to Equation (6):

$$x_{ij} = \sum_{k=1}^p g_{ik} f_{kj} + e_{ij} \quad (6)$$

where  $X_{ij}$  was the content of the  $j$ th element in sample  $i$ ;  $g_{ik}$  represented the relative contribution of the contamination source  $k$  in sample  $i$ ;  $f_{kj}$  was the characteristic value of source  $k$  to concentration of the  $j$ th element;  $e_{ij}$  was the residual; and  $p$  was the number of factors.

### 2.6. Health Risk Assessment

The human exposure health risk assessment model was adopted in health risk assessment in this study, with modifications to some parameters according to the Chinese population. The hazard quotient (HQ) was calculated according to the following formulae:

$$ADD_{ing} = C_s \times \frac{R_{ing} \times EF \times ED}{BW \times AT} \times 10^{-6} \quad (7)$$

$$ADD_{inh} = C_s \times \frac{R_{inh} \times EF \times ED}{PEF \times BW \times AT} \quad (8)$$

$$ADD_{der} = C_s \times \frac{AF \times SA \times ABS \times EF \times ED}{BW \times AT} \times 10^{-6} \quad (9)$$

$$HQ_b = C_b \times \frac{FIR \times EF \times ED}{RfD \times BW \times AT} \quad (10)$$

$$HQ_s = \frac{ADD_{ing}}{RfD_i} \quad (11)$$

where  $C_s$  was the soil HM concentration (mg/kg);  $C_b$  was the HM concentration of bamboo shoots (mg/kg), and the parameters of  $R_{ing}$ ,  $EF$ ,  $ED$ ,  $BW$ ,  $AT$ ,  $R_{inh}$ ,  $AF$ ,  $ABS$ ,  $SA$ ,  $PEF$ ,  $FIR$ , and  $RfD$  are shown in Tables S4 and S5.

The aggregative noncarcinogenic risk associated with multiple exposure routes was represented by the Hazard index (HI, Equation (12)):

$$HI = \sum HQ_i$$

$$x_{ij} = \sum_{k=1}^p g_{ik} f_{kj} + e_{ij} \quad (12)$$

where HI was the total noncarcinogenic health risk index. When the HI value was greater than 1, there was a noncarcinogenic risk to the population.

Finally, the Monte Carlo simulation was employed to characterize the probability distribution of health risks induced by HMs in the study area. The related parameter settings of the Monte Carlo model are presented in Tables S6 and S7.

### 2.7. Statistical Analysis Methods

Data collection and descriptive statistics were conducted with Microsoft Excel 2016, and all data were presented as the means  $\pm$  standard deviations (SD). SPSS 21.0 software was used to perform statistical analyses. The histograms and box plot were handled with Origin 2021. Spatial data interpolation was performed with ArcGis 10.8, and the inverse distance weighting (IDW) method was used in this study.

### 3. Results

#### 3.1. Concentrations and Pollution Assessment of HMs in Soil

##### 3.1.1. Soil HMs Contents

The pH values of soil samples showed that the *D. brandisii* stands mainly occurred in acidic and slightly acidic soil (Table 1). The mean contents of soil HMs in most quadrats were higher than the background values of China and Yunnan, indicating a higher soil background value in the study area. In particular, the mean contents of Cr, Mn, As, and Cd in the study area were 1.34, 1.31, 1.61, and 1.10 times the background value of Yunnan, respectively. On the other hand, the average contents of As, Cu, Ni, Cd, and Cr in the soil samples from 74 quadrats exceeded the soil environmental quality standard of China (Table 1) by 23%, 20%, 16%, 9%, and 8%, respectively. Therefore, special attention should be paid to the risk level assessment and source analysis of key HMs, such as As, Cd, and Cr.

Moreover, except for Pb, the average values of the remaining seven HMs in SF mode were much higher than those in LA mode (Figure S1). The coefficients of variation (CV) of 74 soil samples from two cultivation patterns are shown in Table S8. The pH of soil samples had a low CV value (13.4%–13.7%) in both SF and LA patterns. As for the eight examined HMs, except for Pb, the CV values of the remaining HMs, such as Cr, Ni, and Mn, were higher in the LA than those of the SF pattern. This indicated that the HMs in LA soil samples were more strongly affected by human activities. Moreover, all CV values of As, Ni, Zn, and Cu were more than 100% and exhibited significant differences among quadrats, suggesting that these elements were severely affected by human activities.

##### 3.1.2. Pollution Assessment of HMs

The contamination levels of HMs in soil were evaluated by  $P_i$ ,  $I_{geo}$ , and RI. On average, except for As and Pb, the single pollution index  $P_i$  values of Zn, Cu, Ni, Cr, Mn, and Cd were higher in the SF pattern than those in the LA pattern (Figure 2a). Cr, Ni, Cu, As, and Cd all had some quadrats with  $P_i > 1$ , while  $P_i < 1$  in the values of Zn and Pb. Accordingly, the contents of Cr, Zn, Cu, and Ni in the LA pattern were lower than those in the SF pattern, while the contents of As and Pb were higher in the LA pattern.

The  $I_{geo}$  values of Cr, As, Cd, Mn, Cu, Zn, Ni, and Pb ranged from  $-3.22$  to  $3.81$ , and the mean values were  $-0.39$ ,  $-0.49$ ,  $-0.73$ ,  $-1.01$ ,  $-1.08$ ,  $-1.26$ ,  $-1.44$ ,  $-1.67$  (Figure 2b), respectively. 96%, 92%, 89%, and 88% of soil samples were not polluted by Pb, Zn, Cu, and Ni ( $I_{geo} \leq 0$ ). However, 24.32% of soil samples were mild to moderately contaminated with Cr and As, and 12.16% with Mn and Cd ( $0 < I_{geo} \leq 1$ ), while less than 5% of samples were moderately polluted by multiple HMs ( $1 < I_{geo} \leq 2$ ). On the whole, 85.14% of soil samples had no risk. The element As had a maximum  $I_{geo}$  value ( $I_{geo} = 3.81$ ), which requires special attention. Given that this soil is used for bamboo cultivation and bamboo shoots are used as vegetables, the potential ecological risk may pose a threat to human health. In addition, two cultivation patterns also exhibited different ecological accumulation risks for HMs. Except for As and Pb, the  $I_{geo}$  values of the remaining six HMs were higher under the SF pattern than those under the LA pattern.

The results of RI (Table S11) demonstrated that there were great differences in the range of  $E_r^i$  values and the spatial levels of ecological risk of each HM in the study area. The average values of  $E_r^i$  were 0.81, 0.94, 2.69, 2.86, 4.61, 16.32, and 33.39 for Zn, Mn, Cr, Pb, Cu, As, and Cd, indicating that the overall HMs showed low risk ( $E_r^i < 40$ ). However, 27.03% of samples with moderate risk ( $40 \leq E_r^i < 80$ ) were polluted by Cd, with a maximum value of 207.90. In addition, among the examined HMs, As had the highest  $E_r^i$  value of 214.57. Therefore, Cd and As were the main causes of ecological risk. On the other hand, the RI value ranged from 22 to 306, with an average value of 65.59, indicating a low risk. Cd had the most contribution (54.19%), and the next was As (26.49%). Similarly, in terms of cultivation mode, SF was higher than LA, which was consistent with the results of  $P_i$  and  $I_{geo}$ . Except for Pb, most HM contents were higher in SF than in LA, which was consistent with the results of  $I_{geo}$ .

**Table 1.** The limit standard of China for HMs in soil.

Indices		pH	Content (mg/kg)							
			Cr	Mn	Ni	Cu	Zn	As	Cd	Pb
Background value in China ( <i>n</i> = 4094)	Maximum	-	1209	5888	627	272	593	626	13.4	1143
	Minimum	-	2.20	1	0.06	0.33	2.60	0.01	0.001	0.68
	Mean	-	61.0	583	26.9	22.6	74.2	11.2	0.097	26.0
Background value in Yunnan ( <i>n</i> = 73)	Maximum	8.8	426.0	2768	315.0	208.9	281.0	133.8	3.409	490.0
	Minimum	4.0	13.7	70	4.5	6.2	14.0	1.0	0.009	9.5
	Mean	5.7	65.2	626	42.5	46.3	89.7	18.4	0.218	40.6
This study in LA (bamboo forests of the large-area intensive afforestation pattern) ( <i>n</i> = 34)	Maximum	6.9	135.5	2005.63	57.26	112.62	166.37	62.70	0.70	177.6
	Minimum	3.7	36.64	144.95	8.78	10.29	18.40	8.31	0.06	7.32
	Mean	5.7	67.49	561.05	20.46	34.59	55.43	23.68	0.20	25.31
This study in SF (bamboo forests of the small-scale farmer management pattern) ( <i>n</i> = 40)	Maximum	7.9	458.3	2235.27	265.04	424.88	730.21	388.37	1.51	101.7
	Minimum	4.1	31.56	117.45	7.11	11.56	17.08	8.17	0.05	6.54
	Mean	5.9	104.6	610.46	49.10	49.63	86.89	34.53	0.28	21.39
Based on the soil environmental quality standard of China (GB15618-2018)		pH ≤ 5.5	150		60	50	200	40	0.3	70
		5.5 < pH ≤ 6.5	150		70	50	200	40	0.3	90
		6.5 < pH ≤ 7.5	200		100	100	250	30	0.3	120
		pH > 7.5	250		190	100	300	25	0.6	170

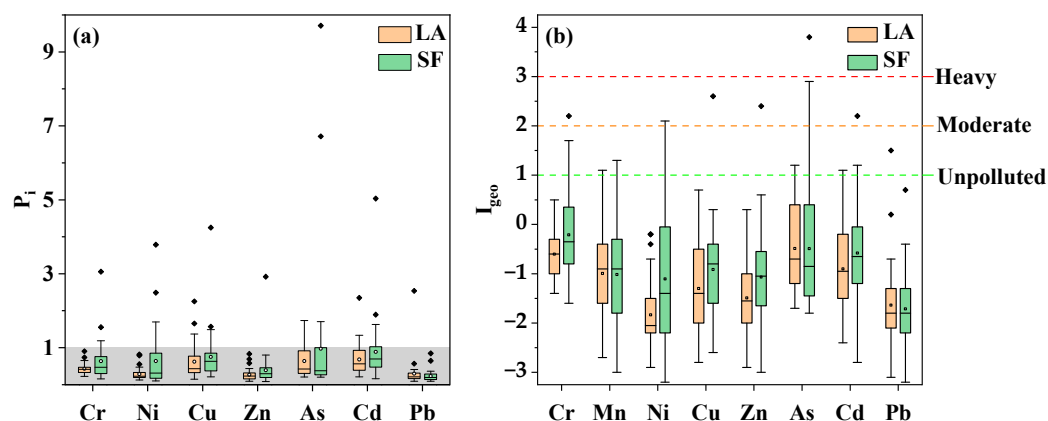


**Figure 2.** The single pollution index ( $P_i$ ) (a) and geoaccumulation index ( $I_{geo}$ ) (b) of seven HMs in LA and SF. LA, bamboo forests of the large-area intensive afforestation pattern; SF, bamboo forests of the small-scale farmer management pattern.

### 3.1.3. Spatial Distribution Characteristics

In this study, Cd, Cr, Cu, Mn, Ni, Pb, Zn, and As all exhibited apparent spatial distribution patterns (Figure S2). The spatial distributions of Cd and As were highly consistent, and these two elements showed significantly higher values in Mojiang. Similarly, Cu and Zn had significantly higher values in Shiping. Additionally, Mojiang and Ninger had high values of Cr and Ni, and the distribution areas with high values of Mn and Pb were Xinping and Shiping, and Shiping and Simao, respectively.

### 3.2. Concentrations of HMs in Bamboo Shoots

The contents of HMs in bamboo shoot samples under two cultivation patterns, namely LA and SF, were determined (Table S10). The mean concentrations of Cd, As, Pb, Ni, Cr, Cu, Zn, and Mn in shoot samples were 0.01, 0.03, 0.07, 0.33, 0.52, 3.40, 5.07, and 6.42 mg/kg, respectively. The results indicated that except for Cr, the average contents of the remaining HMs in the study area did not exceed the limit of the national standard of China (GB2762-2022) (NHCPRC 2022) [35], but the maximum content values for each HM (except for As) exceeded the limit, suggesting that the pollution in the area was generally weak. On the other hand, 7%, 11%, and 39% of shoot samples exceeded the limits of Cd, Pb, and Cr, respectively.

In terms of cultivation pattern, the average contents of HMs in bamboo shoots were not closely related to their habitats. The average contents of Mn, Cr, Zn, and Cu in the LA quadrats were higher than those of the SF quadrats, which was different from the results of soil samples. Overall, the CV values for Ni, As, Cd, and Pb were all 109%, 136%, 170%, and 132%, indicating strong variability in the contents of these HMs among different quadrats in the study area. Those four HMs may be significantly influenced by human activities (Table S11).

### 3.3. Soil Profiles

The concentrations of HMs in five typical soil profiles are presented in Figure S3. The vertical distribution of HM contents did not exhibit a clear correlation with the soil layers. In terms of specific HM elements, Pb consistently showed the highest concentration in layer A among all profiles, with a maximum value of 28.09 mg/kg. Except for profile 3, Cr and Ni had the highest concentrations in layer C, while Cu had the lowest concentration in layer C among the remaining profiles, with a minimum value of 12.49 mg/kg. Additionally, except for profile 2, the vertical distribution of Mn in the soil displayed a decreasing trend with soil layer depth. These results suggested that Pb, Cu, and Mn may be significantly influenced by anthropogenic pollution.

Additionally, with regard to cultivation patterns, the HM contents at each layer of profiles 1–3 (under the SF pattern) exceeded the permissible limits, whereas HM concen-

trations in each layer of profiles 4 and 5 (from the LA pattern) were below the national standards (Figure S3). In particular, Cd content in all three soil layers exceeded the standard limits in profile 1, and As content in all three soil layers also exceeded the standard limits in profiles 2 and 3.

### 3.4. Correlation Analysis of HMs between Bamboo Shoots and Soil

The present study revealed strong and complex correlations among different HMs in bamboo shoots and soil. Specifically, Cr exhibited significantly positive correlations with Cu and negative correlations with As and Cd ( $p < 0.001$ ) (Figure 3a). Zn exhibited highly significant positive correlations with Cd, Ni, Pb, and Mn, while As demonstrated a significantly negative correlation with Cu, and Cd exhibited significantly positive correlations with Zn, Mn, and Pb. Pb showed a significantly positive correlation with Cd, As, and Zn.

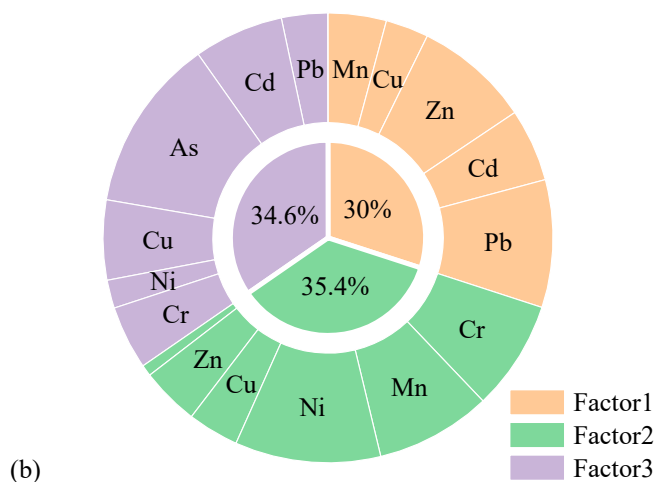
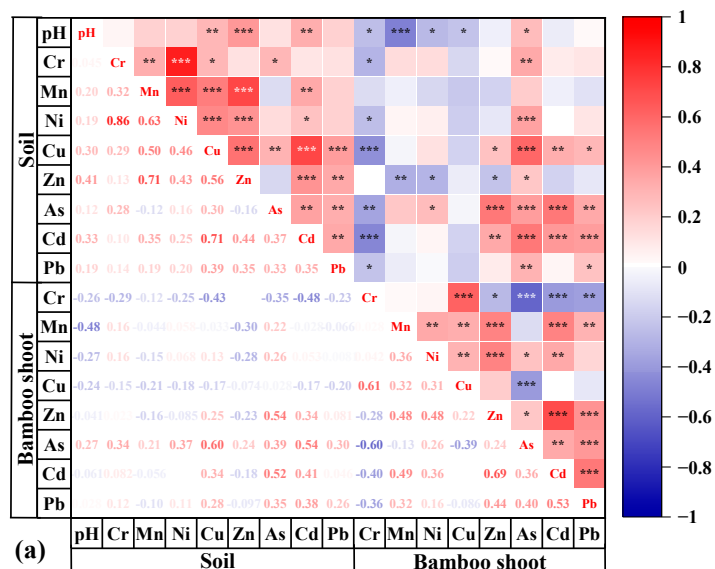


**Figure 3.** Analysis of HM sources. (a) Correlation of HMs between bamboo shoots and soil ( $* p \leq 0.05$ ,  $** p \leq 0.01$ , and  $*** p \leq 0.001$ ) and (b) the contribution of HMs to each factor.

Among the soil samples, Ni exhibited a significantly positive correlation with Cr ( $R = 0.86$ ), and Cu also showed a significantly positive correlation with Cd ( $R = 0.71$ ). Additionally, Cu had positive correlations with Pb, Mn, Zn, and Ni ( $p < 0.001$ ), and Zn exhibited positive correlations with Pb, Mn, Cu, Cd, and Ni ( $p < 0.001$ ).

Furthermore, significantly positive correlations of HM contents between soil samples and bamboo shoot samples were found in both As and Cd. This suggested that the

concentrations of HMs in the soil may influence the bioaccumulation of these elements in bamboo shoots to some extent.

### 3.5. Source Apportionment of HMs

The PMF model was used to identify the major sources of heavy metal(loid)s and quantify their contributions. In the PMF model analysis, an acceptable confidence level (minimum Q) was found when the factor number was set to 3. There was a good correlation between the measured and predicted values for all elements, with  $R^2 > 0.61$  (Figure S4). This indicated that the parameter selection of the PMF model was reasonable, and the results were reliable, providing a good explanation for the sources of HMs in the study area soil. The results revealed that the sources of HMs in the soil of bamboo cultivation areas could be classified into three factors (Figure 3b). The contributions of factors 1, 2, and 3 were 30%, 35.4%, and 34.6%, respectively. The profile of the three factors and the contribution of each HM to soil pollution in the PMF model were presented in Figures S5–S7. Pb and Zn were the main loading elements for Factor 1, with 30.57% and 27.72% contributions, respectively. Factor 2 was primarily influenced by Ni, Mn, and Cr, contributing 29.62%, 23.52%, and 22.37%, respectively. In Factor 3, As was the key loading element with a 36.09% contribution.

### 3.6. Health Risk Assessment

The analysis results of HQ showed that the adult values (HQa) of all eight HMs were less than 1, indicating that the HM content in the bamboo shoots of *D. brandisii* in the study area posed a low health risk to adults (Figure 4a). Except for As and Pb, LA has lower health risks than SF. It was noteworthy that HQ of As for children in some shoot samples exceeded 1, and suggested a potential health risks to children (Figure 4b).

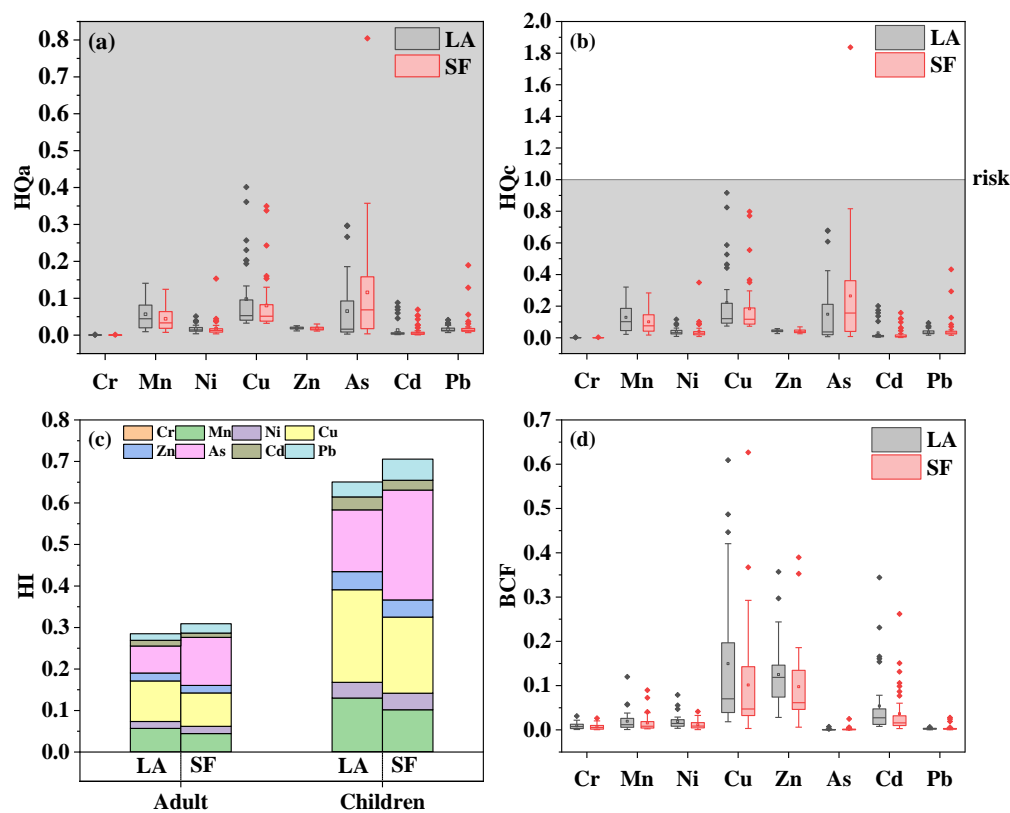


**Figure 4.** Assessment results of HMs contamination in bamboo shoots by hazard quotient for adults (HQa) (a), hazard quotient for children (HQc) (b), hazard index (Hi) (c) and Bioconcentration factor (BCF) (d). LA, bamboo forests of the large-area intensive afforestation pattern; SF, bamboo forests of the small-scale farmer management pattern.

Meanwhile, the HI analysis of HMs in bamboo shoots under two cultivation patterns indicated that HI values were clearly different between adults and children (Figure 4c). The HI values for adults ranged from 0.09 to 0.92, while the HI values for children were 0.21–2.09, indicating a greater health risk for children from bamboo shoots in the study area. Among the average HI values of examined HMs, three elements with the most contribution were: As accounted for 37.49% contribution in SF pattern and 22.87% contribution in LA pattern, Cu was 25.97% in SF and 34.27% in LA, and Mn was 14.31% in SF and 19.86% in LA. Therefore, the main concern for the HM elements was As, Cu, and Mn.

As for the HM accumulation degree in bamboo shoots, the BCF values in bamboo shoot samples (Figure 4d) were Cu (0.123) > Zn (0.110) > Cd (0.045) > Mn (0.017) > Ni (0.015) > Cr (0.008) > Pb (0.003) > As (0.001). This result indicated that bamboo shoots had a low bioaccumulation ability of HMs. By comparison, the BCF values of HMs were higher under LA conditions than those under SF, indicating that the ability of *D. brandisii* to accumulate HMs may be influenced by cultivation conditions.

According to the results of the Monte Carlo simulation, the cumulative probability distribution of health risks induced by HM in bamboo shoots is shown in Figure 5. Among the eight examined HMs, the health risks posed to children were generally greater than those to adults. The simulated HQ values for Mn, Cr, Zn, and Pb were below 1. However, for Ni, Cu, As, and Cd, there was a probability of less than 5% exceeding the health risk threshold of 1. The summation of HQ values for each element and the results of HI indicated significant health risks associated with HMs in bamboo shoots for children, with a 24.82% probability of total noncarcinogenic risk ( $HI_c = 1$ ).

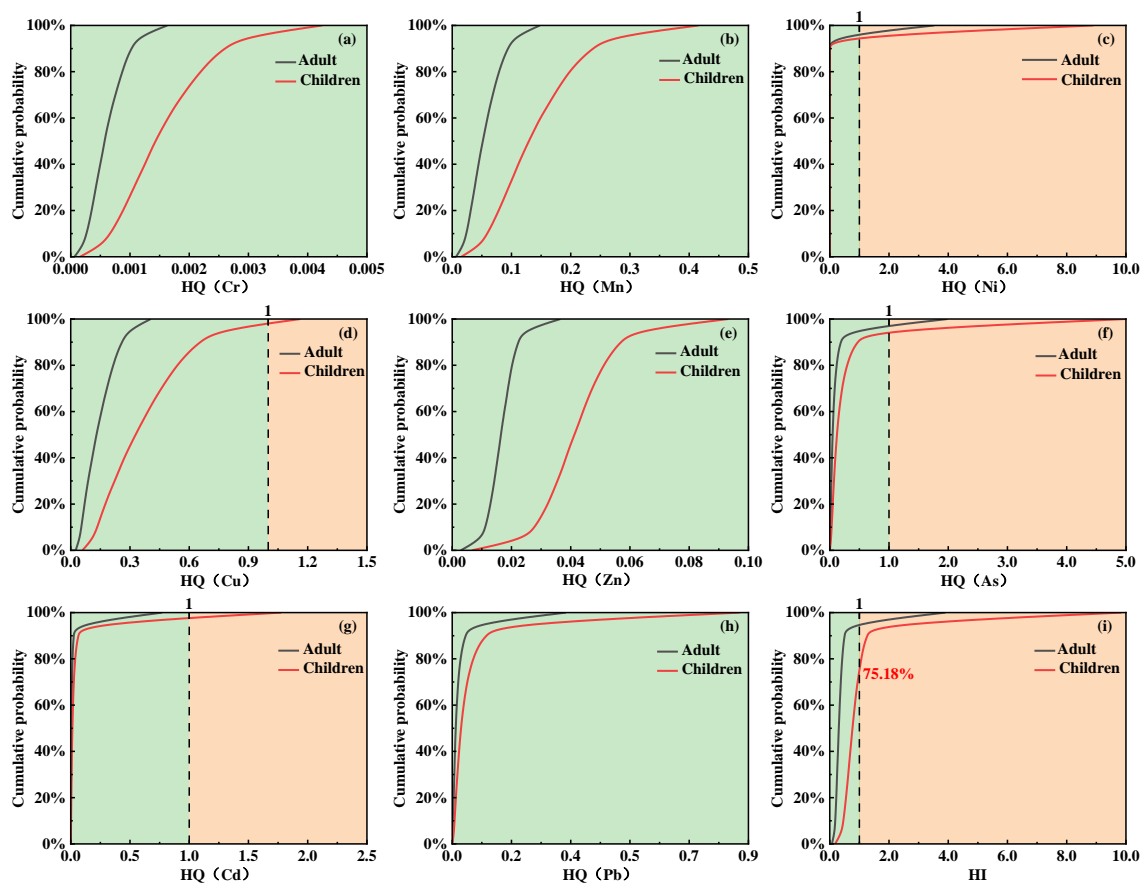


**Figure 5.** Probability distribution of hazard index (HI) and hazard quotient (HQ) for children and adults by bamboo shoots. HQ for Cr (a), Mn (b), Ni (c), Cu (d), Zn (e), As (f), Cd (g), Pb (h), and HI (i).

The probability distributions of HI and HQ in the soil are shown in Figure 6. Similar to bamboo shoots, among the eight HMs, the accumulation risk of HMs in the soil of

the study area was higher in children than in adults. The simulated HQ values for Cd, Zn, Cu, and Ni were below 1, indicating negligible health risks to humans. Both Mn and Pb had a probability of less than 5% to exceed 1, indicating a minimal risk. For Cr, a 12.25% probability of the HQc values for children exceeds 1, suggesting a health risk associated with Cr in children. As has a 13.94% probability of HQc values exceeding 1, indicating a significant health risk to children associated with As in the study area. In the Monte Carlo simulation, over 60.64% of the HI values posed health risks to children, while the probability for adults to experience health risks was less than 5%. The element As contributed significantly to the HI values, making it the primary driver of health risks associated with soil HMs.

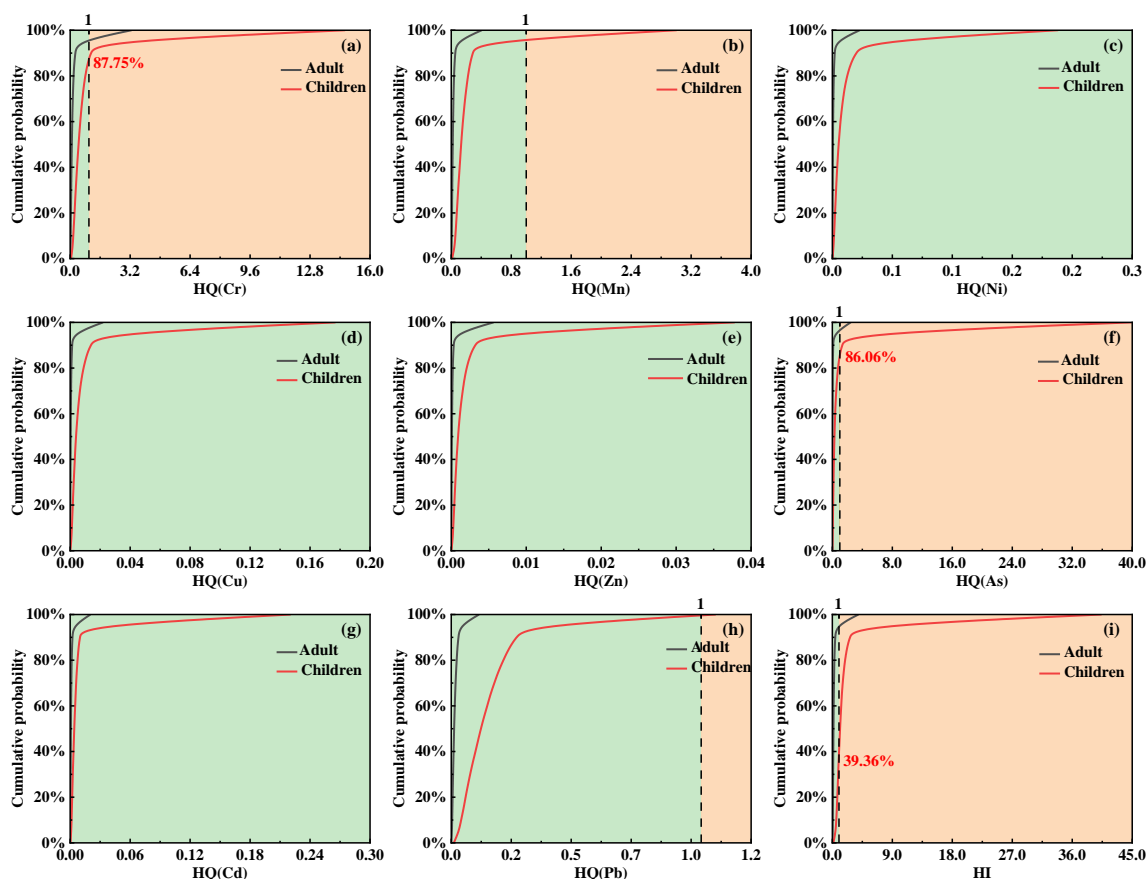


**Figure 6.** Probability distribution of hazard index (HI) and hazard quotient (HQ) for children and adults by soil. HQ for Cr (a), Mn (b), Ni (c), Cu (d), Zn (e), As (f), Cd (g), Pb (h) and HI (i).

#### 4. Discussion

##### 4.1. HM Accumulation and Pollution in Bamboo Shoots and Soil under Two Cultivation Patterns

Based on the combined geo-spatial analysis and multi-pollution index analysis, this study was the first comprehensive research on the accumulation and pollution of HMs in planting areas of *D. brandisii*, an important tropical bamboo, under two cultivation patterns in Yunnan, China. The results indicated that the mean concentrations of HMs in the soil of the examined bamboo stands were higher than the background values of Yunnan [7,8]. In particular, the average concentrations of As, Cr, Mn, and Cd were higher than their background values by 1.61, 1.34, 1.31, and 1.10 times [5]. On the other hand, the mean contents of Cr in bamboo shoots in the study area also exceeded the background values of the study area. Furthermore, 39%, 11%, and 7% of the shoot samples went beyond the limits of Cr, Pb, and Cd, respectively. Therefore, special attention should be paid to the potential pollution risk and source of Cr, Pb, and Cd in bamboo shoots.

Currently, SF and LA are two typical cultivation and management patterns for *D. brandisii* in Yunnan [28,29]. In the soil of the cultivation area, except for Pb, the mean contents of HMs in the SF pattern were generally higher than those in the LA pattern. This suggested that human activities have a greater impact on the content of HMs in the soil and bamboo shoots [36]. The LA pattern, with minimal human intervention, may help reduce the accumulation and pollution of HMs, while the SF model has led to the noteworthy accumulation of HMs because of human disturbances and the use of fertilizers to achieve higher yields and quality of bamboo shoots [3,37]. Therefore, in the cultivation of *D. brandisii*, the HM pollution threats caused by anthropogenic activities such as fertilizer application should be reduced as much as possible [38].

#### 4.2. HM Source Apportionment in Soil of Cultivation Areas of *D. brandisii*

The global HMs in agricultural and forest soils basically originate from human activities and natural sources [7,21,23]. The results of the PMF model showed that the sources of HMs in the soil of bamboo cultivation areas could be classified into three factors (Figure 3b). Factor 1 was significantly correlated with Pb and Zn. It was well documented that traffic and transportation activities were closely linked to Pb contamination in soil [1,2,39]. Moreover, brake wear, tire abrasion, and tear, as well as exhaust emissions from vehicles using leaded fuel or those containing Zn additives, could contribute to Pb and Zn pollution of the soil [40,41]. Therefore, Factor 1 was considered to be a traffic-related source.

Meanwhile, Factor 2 was strongly correlated with Ni, Mn, and Cr (Figure 3b). These elements were commonly existed in soil parent materials and were major components of soil formation. Therefore, their presence can be attributed to natural sources rather than human activities. Previous studies had also indicated that the accumulations of Cr, Mn, and Ni in soil were mainly affected by the parent rock [42,43]. Additionally, the analysis of soil profiles (Figure S3) showed that Ni and Cr exhibited the highest concentrations at deeper depths, which was consistent with the high HM geological background of Yunnan [6,8]. Hence, Factor 2 was probably associated with natural sources.

Factor 3 was predominantly influenced by As, suggesting this element originated from mining and metal smelting activities (Figure 3b). Yunnan is known for its abundant mineral resources, including gold, copper, lead, zinc, tin, etc. [44]. Central Yunnan was renowned for its abundant gold deposits [45]. The long-term mining activities in the study area could lead to the enrichment of As in the soil [46,47]. In this study, soil Profile 2 and Profile 3 near an active gold mine exhibited significantly high As concentrations in all soil layers; even the As content of the surface soil in Profile 3 was 1.7 times higher than the permissible limit (Figure S3). This confirmed that mining and metal smelting activities were the main sources of As in the study area.

#### 4.3. Risk Assessment of HMs in Soil and Bamboo Shoots

With the prosperity in industry and mining and the excessive use of dirty irrigation, the soils and crops of some farmlands and forestlands in the arid zone of China have accumulated a large number of HMs [48]. In this study, the investigated area was characterized by a developed mining industry and high background values of soil HMs, thus posing a potential threat to human health and the ecological environment [45,47]. Fortunately, our results indicated that the bamboo shoots of *D. brandisii* had a low health risk to adults based on the HM content in the study area (Figure 4a). However, 24.82% of the shoot samples had a probability of the HI value exceeding 1, indicating potential health risks to children. Likewise, although the overall average value of the RI of shoot samples in the study area suggested a low risk, the maximum value of the RI in shoot samples reached a high-risk level, with significant contributions from Cd and As. Meanwhile, As also had the maximum values of  $P_i$  and  $I_{geo}$  in the soil samples. Furthermore, the contents of both Cd and As in bamboo shoot samples demonstrated a significantly positive correlation with their contents in soil samples (Figure 3). Actually, As was a key HM of concern in mining areas [49], and Cd was also a major monitoring pollutant in agricultural and forestry soils in

China [50]. In addition, the average value of Cr in soil samples exceeded the limit value of China, and the Cr contents of 39% of shoot samples were higher than the limits of China's national criterion. Cr in soil is predominantly derived from the parent material in the soil formation process [51]. Therefore, it is important to detect soil physical and chemical properties before bamboo cultivation so as to avoid selecting land of the soils with a high Cr content as a plantation.

Based on the Monte Carlo simulation, we identified the noncarcinogenic risk of HMs in both the soil and bamboo shoots in the study area and found that children generally had a higher HI compared to adults and were more susceptible to risks associated with HMs. In this study, children had potential health risks with a probability of HI > 60.64%, while HI < 5% was for adults. Previous studies have also indicated that children were more vulnerable to the effects of toxic substances compared to adults, mainly because of their physiological characteristics, intake level, and exposure duration [36]. The elements As and Cu contributed significantly to the HI values in this index (Figure 4c) and were the primary drivers of health risks associated with soil HMs. Therefore, to control health risks for children in the study area, Cu and As should be taken seriously.

## 5. Conclusions

The present study revealed that soil HM concentrations of the *D. brandisii* stands in the study area were higher than the background values of Yunnan. On the whole, the mean contents of HMs in the SF pattern were generally higher than those in the LA pattern. At the same time, a relatively low ecological risk level was detected in the study area, and Cd and As were identified as the main contributors to ecological risk. The ability of bamboo shoots to accumulate HMs from the soil was generally low, and Cu and Zn were the two most easily accumulated elements in bamboo shoots in the study area. On the other hand, soil HMs in the study area could be classified into three main sources, including natural sources from pedogenic parent material for Ni, Mn, and Cr; mining and metallurgical activities for As; and traffic emissions for Pb and Zn. Except for As and Pb, LA has lower HQ risks than the SF pattern. Monte Carlo simulations revealed that more than 24.82% of the HI for bamboo shoots exceeded the acceptable limits for children. In particular, As was identified as the most important cause of health risks associated with HM contamination in the study area and should be given priority attention.

**Supplementary Materials:** The following supporting information can be downloaded at <https://www.mdpi.com/article/10.3390/f15010041/s1>, Table S1: The classification of the contamination degree according to the value of  $P_i$  and  $P_N$ . Table S2:  $I_{geo}$  and pollution status of heavy metals. Table S3: Grades of the potential ecological risk index. Table S4: Input parameters to characterize the daily exposure dose of toxic metals via various exposure pathways [52–56]. Table S5: Values of the reference dose (RfD; mg/kg/day) and the slope factor (SF; per mg/kg/day) for HMs [16,57–60]. Table S6: Uncertain parameters of this study's HMs concentrations in soils and bamboo shoots. Table S7: Parameters for human health risk assessment by Monte Carlo simulation [61,62]. Table S8: Coefficient of variation of heavy metal content in different areas in soil. Table S9: Potential ecological risk index and evaluation of ecological risk index of single heavy metals in the study area. Table S10: Heavy metals content in bamboo shoots ( $n = 74$ ). Table S11: Coefficient of variation of heavy metal content in different areas in bamboo shoots. Figure S1: Heavy metal content of Cr, Mn, Ni, Cu, Zn, As, Cd, and Pb from different bamboo shoot areas. Figure S2: Spatial distribution of heavy metals content in the research area. Figure S3: Heavy metal content in soil profiles (mg/kg). Figure S4: Fitting coefficients ( $r^2$ ) of measured and predicted HMs concentrations in soil. Figure S5: Contribution of heavy metal elements in each factor. Figure S6: Profile of three factors and contribution of each HM to soil contamination. Figure S7: Factor contribution of heavy metals in soil by PMF model.

**Author Contributions:** Q.C.: Software, Methodology, Formal analysis, and Writing—original draft. P.D.: Formal analysis and Investigation. C.B.: Conceptualization, Formal analysis, and Writing—original draft. Z.Z.: Formal analysis and Investigation. Y.C.: Formal analysis and Investigation. H.Y.: Conceptualization, Funding acquisition, Supervision, and Writing—review and editing. All authors have read and agreed to the published version of the manuscript.

**Funding:** This research was funded by the Fundamental Research Funds of the Chinese Academy of Forestry (No. CAFYBB2021SZ001), the National Natural Science Foundation of China (No. 31870574), the Department of Sciences and Technology of Xizang Autonomous Region (No. XZ201801-GA-11), and Yunnan Forestry Technological College (KY(TD)202202).

**Data Availability Statement:** The datasets used in the study are available from the corresponding author upon reasonable request.

**Conflicts of Interest:** The authors declare no conflict of interest.

## References

1. Szwalec, A.; Mundala, P.; Kedzior, R.; Pawlik, J. Monitoring and Assessment of Cadmium, Lead, Zinc and Copper Concentrations in Arable Roadside Soils in Terms of Different Traffic Conditions. *Environ. Monit. Assess.* **2020**, *192*, 155. [[CrossRef](#)] [[PubMed](#)]
2. Feng, J.F.; Wang, Y.X.; Zhao, J.; Zhu, L.Q.; Bian, X.M.; Zhang, W.J. Source Attributions of Heavy Metals in Rice Plant along Highway in Eastern China. *J. Environ. Sci.* **2011**, *23*, 1158–1164. [[CrossRef](#)] [[PubMed](#)]
3. Cao, C.; Chen, X.P.; Ma, Z.B.; Jia, H.H.; Wang, J.J. Greenhouse Cultivation mitigates Metal-Ingestion-Associated Health Risks from Vegetables in Wastewater-Irrigated Agroecosystems. *Sci. Total Environ.* **2016**, *560*, 204–211. [[CrossRef](#)] [[PubMed](#)]
4. Rahman, Z.; Singh, V.P. The Relative Impact of Toxic Heavy Metals (THMs) (Arsenic (As), Cadmium (Cd), Chromium (Cr)(VI), Mercury (Hg), and Lead (Pb)) on the Total Environment: An Overview. *Environ. Monit. Assess.* **2019**, *191*, 419. [[CrossRef](#)] [[PubMed](#)]
5. SEPB; CNEMC. *Background Values of Soil Elements in China*; China Environmental Science Press: Beijing, China, 1990; pp. 87–485.
6. Yang, M.; He, L.; Zeng, P.; He, S.; Yang, T. Evaluation and Migration Law of Heavy Metal Pollution in River Sediment of a Copper Mining Area in Yunnan. *J. Anhui Agric. Sci.* **2023**, *51*, 68–72.
7. Zhong, T.Y.; Xue, D.W.; Zhao, L.M.; Zhang, X.Y. Concentration of Heavy Metals in Vegetables and Potential Health Risk Assessment in China. *Environ. Geochem. Health* **2018**, *40*, 313–322. [[CrossRef](#)] [[PubMed](#)]
8. Hu, B.F.; Shao, S.; Ni, H.; Fu, Z.Y.; Hu, L.S.; Zhou, Y.; Min, X.X.; She, S.F.; Chen, S.C.; Huang, M.X.; et al. Current Status, Spatial Features, Health Risks, and Potential Driving Factors of Soil Heavy Metal Pollution in China at Province Level. *Environ. Pollut.* **2020**, *266*, 114961. [[CrossRef](#)]
9. Dou, P.; Cheng, Q.; Liang, N.; Bao, C.; Zhang, Z.; Chen, L.; Yang, H. Rhizosphere Microbe Affects Soil Available Nitrogen and Its Implication for the Ecological Adaptability and Rapid Growth of *Dendrocalamus Sinicus*, the Strongest Bamboo in the World. *Int. J. Mol. Sci.* **2023**, *24*, 14665. [[CrossRef](#)]
10. Zhan, F.D.; Zeng, W.Z.; Yuan, X.C.; Li, B.; Li, T.G.; Zu, Y.Q.; Jiang, M.; Li, Y. Field Experiment on the Effects of Sepiolite and Biochar on the Remediation of Cd- and Pb-Polluted Farmlands around a Pb-Zn Mine in Yunnan Province, China. *Environ. Sci. Pollut. Res.* **2019**, *26*, 7743–7751. [[CrossRef](#)]
11. Wang, F.; Zhao, W.J.; Chen, Y.Y. Spatial Variations of Soil Heavy Metal Potential Ecological Risks in Typical Moso Bamboo Forests of Southeast China. *Bull. Environ. Contam. Toxicol.* **2019**, *102*, 224–230. [[CrossRef](#)]
12. Soleimani, H.; Mansouri, B.; Kiani, A.; Omer, A.K.; Tazik, M.; Ebrahimzadeh, G.; Sharafi, K. Ecological Risk Assessment and Heavy Metals Accumulation in Agriculture Soils Irrigated with Treated Wastewater Effluent, River Water, and Well Water Combined with Chemical Fertilizers. *Heliyon* **2023**, *9*, e14580. [[CrossRef](#)] [[PubMed](#)]
13. Zhou, W.X.; Han, G.L.; Liu, M.; Song, C.; Li, X.Q.; Malem, F. Vertical Distribution and Controlling Factors Exploration of Sc, V, Co, Ni, Mo and Ba in Six Soil Profiles of the Mun River Basin, Northeast Thailand. *Int. J. Environ. Res. Public Health* **2020**, *17*, 1745. [[CrossRef](#)] [[PubMed](#)]
14. Wei, W.; Li, X.N.; Ling, S.X.; Wu, X.Y.; Liao, X. Heavy Metal (Loid) and Pb Isotope Compositions of Black Shale Weathering Profiles on the Northern Yangtze Platform: Insights into Geochemical Behavior, Contamination Assessment, and Source Apportionment. *Environ. Sci. Pollut. Res.* **2021**, *28*, 50230–50244. [[CrossRef](#)] [[PubMed](#)]
15. Gui, R.Y.; Hu, Y.Y.; Li, Q.; Zhuang, S.Y. Effect of Cultivation Time on Soil Heavy Metal Accumulation and Bioavailability in *Phyllostachys Praecox* Stands. *Pedosphere* **2020**, *30*, 810–816. [[CrossRef](#)]
16. Mo, R.; Cheng, J.; Tang, F.; Yue, J.; Li, Z.; Ni, Z. Heavy Metals in Bamboo Shoots from Southeastern China and Risk Assessment. *Food Addit. Contam. Part B* **2021**, *14*, 264–270. [[CrossRef](#)]
17. Wang, Z.H.; Chen, Y.L.; Wang, S.; Yu, Y.J.; Huang, W.Y.; Xu, Q.L.; Zeng, L. Pollution Risk Assessment and Sources Analysis of Heavy Metal in Soil from Bamboo Shoots. *Int. J. Environ. Res. Public Health* **2022**, *19*, 14806. [[CrossRef](#)] [[PubMed](#)]
18. Yang, Q.F.; Wang, S.L.; Zhao, C.C.; Nan, Z.R. Risk Assessment of Trace Elements Accumulation in Soil-Herbage Systems at Varied Elevation in Subalpine Grassland of Northern Tibet Plateau. *Environ. Sci. Pollut. Res.* **2022**, *29*, 27636–27650. [[CrossRef](#)]
19. Susana, F.; Tomás, C.Y.; Javier, R.P.; Celestino, O. Geographically Weighted Principal Components Analysis to Assess Diffuse Pollution Sources of Soil Heavy Metal: Application to Rough Mountain Areas in Northwest Spain. *Geoderma* **2018**, *311*, 120–129. [[CrossRef](#)]
20. Yaseen, Z.M. The next Generation of Soil and Water Bodies Heavy Metals Prediction and Detection: New Expert System Based Edge Cloud Server and Federated Learning Technology. *Environ. Pollut.* **2022**, *313*, 120081. [[CrossRef](#)]
21. Xiang, M.T.; Li, Y.; Yang, J.Y.; Lei, K.G.; Li, Y.; Li, F.; Zheng, D.F.; Fang, X.Q.; Cao, Y. Heavy Metal Contamination Risk Assessment and Correlation Analysis of Heavy Metal Contents in Soil and Crops. *Environ. Pollut.* **2021**, *278*, 116911. [[CrossRef](#)]

22. Heidari, M.; Darijani, T.; Alipour, V. Heavy Metal Pollution of Road Dust in a City and Its Highly Polluted Suburb; Quantitative Source Apportionment and Source-Specific Ecological and Health Risk Assessment. *Chemosphere* **2021**, *273*, 129656. [[CrossRef](#)] [[PubMed](#)]
23. Zulkafflee, N.S.; Mohd Redzuan, N.A.; Nematbakhsh, S.; Selamat, J.; Ismail, M.R.; Praveena, S.M.; Yee Lee, S.; Abdull Razis, A.F. Heavy Metal Contamination in *Oryza Sativa* L. at the Eastern Region of Malaysia and Its Risk Assessment. *Int. J. Environ. Res. Public Health* **2022**, *19*, 739. [[CrossRef](#)] [[PubMed](#)]
24. Thompson, K.M.; Burmaster, D.E.; Crouch, E.A. Monte Carlo Techniques for Quantitative Uncertainty Analysis in Public Health Risk Assessments. *Risk Anal. Off. Publ. Soc. Risk Anal.* **1992**, *12*, 53–63. [[CrossRef](#)] [[PubMed](#)]
25. Guo, P.; Li, H.M.; Zhang, G.M.; Tian, W. Contaminated Site-Induced Health Risk Using Monte Carlo Simulation: Evaluation from the Brownfield in Beijing, China. *Environ. Sci. Pollut. Res.* **2021**, *28*, 25166–25178. [[CrossRef](#)] [[PubMed](#)]
26. Chen, X.P.; Liu, S.Y.; Luo, Y. Spatiotemporal Distribution and Probabilistic Health Risk Assessment of Arsenic in Drinking Water and Wheat in Northwest China. *Ecotoxicol. Environ. Saf.* **2023**, *256*, 114880. [[CrossRef](#)] [[PubMed](#)]
27. Li, X.F.; Fu, B.T.; Guo, J.; Ji, K.L.; Xu, Y.K.; Dahab, M.M.; Zhang, P. Bamboo Shoot Fiber Improves Insulin Sensitivity in High-Fat Diet-Fed Mice. *J. Funct. Foods* **2018**, *49*, 510–517. [[CrossRef](#)]
28. Yang, H.Q.; Sun, M.S.; Ruan, Z.Y.; Dong, Y.R.; Liang, N. Study on Provenance Differentiation of Four Typical Tropical Clump bamboos in Yunnan, China. *For. Res.* **2014**, *27*, 168–173.
29. Hui, C.M.; Liu, W.Y.; Zhang, G.X.; Shi, M.; Lu, D.W.; Zou, X.M. Exploration and Breeding of Excellent Germplasm Resources of Sweet Dragon Bamboo. *J. Bamboo* **2019**, *38*, 26–30.
30. Bahru, T.; Ding, Y.L. Effect of Stand Density, Canopy Leaf Area Index and Growth Variables on *Dendrocalamus Brandisii* (Munro) Kurz Litter Production at Simao District of Yunnan Province, Southwestern China. *Glob. Ecol. Conserv.* **2020**, *23*, e01051. [[CrossRef](#)]
31. Chen, J.; Zhang, J.L.; Qu, M.K.; Yang, L.F.; Zhao, Y.C.; Huang, B. Pollution Characteristics and Risk Assessment of Soil Heavy Metals in the Areas Affected by the Mining of Metal-Bearing Minerals in Southwest China. *Bull. Environ. Contam. Toxicol.* **2021**, *107*, 1070–1079. [[CrossRef](#)]
32. GB15618-2018; Soil Environmental Quality—Risk Control Standard for Soil Contamination of Agricultural Land. MEE (Ministry of Ecology and Environment): Beijing, China, 2018. (In Chinese)
33. Hakanson, L. An Ecological Risk Index for Aquatic Pollution Control. A Sedimentological Approach. *Water Res.* **1980**, *14*, 975–1001. [[CrossRef](#)]
34. Moya, J. *Exposure Factors Handbook*; Exposure Analysis and Risk Characterization Group, US EPA National Center for Environmental Assessment: Washington, DC, USA, 1997.
35. GB2762-2022; National Standards for Food Safety. NHC (National Health Commission of the People’s Republic of China): Beijing, China, 2022. (In Chinese)
36. Liang, J.; Liu, Z.; Tian, Y.; Shi, H.; Fei, Y.; Qi, J.; Mo, L. Research on Health Risk Assessment of Heavy Metals in Soil Based on Multi-Factor Source Apportionment: A Case Study in Guangdong Province, China. *Sci. Total Environ.* **2023**, *858*, 159991. [[CrossRef](#)] [[PubMed](#)]
37. Yu, H.L.; Shen, X.F.; Chen, H.Y.; Dong, H.R.; Zhang, L.J.; Yuan, T.; Zhang, D.; Shang, X.D.; Tan, Q.; Liu, J.Y.; et al. Analysis of Heavy Metal Content in *Lentinula Edodes* and the Main Influencing Factors. *Food Control* **2021**, *130*, 108198. [[CrossRef](#)]
38. Zhang, S.C.; Zhao, R.; Wu, K.; Huang, Q.; Kang, L. Effects of the Rapid Construction of a High-Quality Plough Layer Based on Woody Peat in a Newly Reclaimed Cultivated Land Area. *Agriculture* **2022**, *12*, 31. [[CrossRef](#)]
39. Lee, H.; Byun, Y.J.; Chun, Y.; Noh, H.; Kim, D.; Kim, H.; Kim, J. Identification of Metal Contamination Sources and Evaluation of the Anthropogenic Effects in Soils near Traffic-Related Facilities. *Toxics* **2021**, *9*, 278. [[CrossRef](#)] [[PubMed](#)]
40. Superville, P.J.; Prygiel, E.; Magnier, A.; Lesven, L.; Gao, Y.; Baeyens, W.; Ouddane, B.; Dumoulin, D.; Billon, G. Daily Variations of Zn and Pb Concentrations in the Defile River in Relation to the Resuspension of Heavily Polluted Sediments. *Sci. Total Environ.* **2014**, *470*, 600–607. [[CrossRef](#)] [[PubMed](#)]
41. Jeong, H.; Ryu, J.; Ra, K. Characteristics of Potentially Toxic Elements and Multi-Isotope Signatures (Cu, Zn, Pb) in Non-Exhaust Traffic Emission Sources. *Environ. Pollut.* **2022**, *292*, 118339. [[CrossRef](#)]
42. Mistikawy, J.A.; Mackowiak, T.J.; Butler, M.J.; Mischenko, I.C.; Cernak, R.S., Sr.; Richardson, J.B. Chromium, Manganese, Nickel, and Cobalt Mobility and Bioavailability from Mafic-to-Ultramafic Mine Spoil Weathering in Western Massachusetts, USA. *Environ. Earth Sci.* **2020**, *42*, 3263–3279. [[CrossRef](#)]
43. Garnier, J.; Quantin, C.; Raous, S.; Guimaraes, E.; Becquer, T. Field Availability and Mobility of Metals in Ferralsols Developed on Ultramafic Rock of Niquelandia, Brazil. *Braz. J. Geol.* **2021**, *51*, e20200092. [[CrossRef](#)]
44. Li, B.; Deng, J.; Li, Z.; Chen, J.; Zhan, F.; He, Y.; He, L.; Li, Y. Contamination and Health Risk Assessment of Heavy Metals in Soil and Ditch Sediments in Long-Term Mine Wastes Area. *Toxics* **2022**, *10*, 607. [[CrossRef](#)]
45. Zhang, Q.; Zhang, F.F.; Huang, C.M. Heavy Metal Distribution in Particle Size Fractions of Floodplain Soils from Dongchuan, Yunnan Province, Southwest China. *Environ. Monit. Assess.* **2021**, *193*, 54. [[CrossRef](#)] [[PubMed](#)]
46. Zhuang, F.; Huang, J.Y.; Li, H.G.; Peng, X.; Xia, L.; Zhou, L.; Zhang, T.; Liu, Z.H.; He, Q.; Luo, F.; et al. Biogeochemical Behavior and Pollution Control of Arsenic in Mining Areas: A Review. *Front. Microbiol.* **2023**, *14*, 1043024. [[CrossRef](#)] [[PubMed](#)]
47. Barago, N.; Mastroianni, C.; Pavoni, E.; Floreani, F.; Parisi, F.; Lenaz, D.; Covelli, S. Environmental Impact of Potentially Toxic Elements on Soils, Sediments, Waters, and Air Nearby an Abandoned Hg-Rich Fahlore Mine (Mt. Avanza, Carnic Alps, NE Italy). *Environ. Sci. Pollut. Res.* **2023**, *30*, 63754–63775. [[CrossRef](#)] [[PubMed](#)]

48. Wu, Y.F.; Li, X.; Yu, L.; Wang, T.; Wang, J.; Liu, T. Review of Soil Heavy Metal Pollution in China: Spatial Distribution, Primary Sources, and Remediation Alternatives. *Resour. Conserv. Recycl.* **2022**, *181*, 106261. [[CrossRef](#)]
49. Shi, J.D.; Zhao, D.; Ren, F.T.; Huang, L. Spatiotemporal Variation of Soil Heavy Metals in China: The Pollution Status and Risk Assessment. *Sci. Total Environ.* **2023**, *871*, 161768. [[CrossRef](#)] [[PubMed](#)]
50. Li, X.; Li, Y.P.; Kang, X.R.; Yu, J.P.; Gao, S.; Zhang, J.; Wang, H.; Pan, H.; Yang, Q.G.; Zhuge, Y.P.; et al. Effective Utilization of Weak Alkaline Soils with Cd-Contamination by Wheat and Rape Intercropping. *Ecotoxicol. Environ. Saf.* **2022**, *248*, 114335. [[CrossRef](#)]
51. Gololobova, A.; Legostaeva, Y. An Assessment of the Impact of the Mining Industry on Soil and Plant Contamination by Potentially Toxic Elements in Boreal Forests. *Forests* **2023**, *14*, 1641. [[CrossRef](#)]
52. US EPA. *Exposure Factors Handbook: 2011 Edition*; EPA/600/R-09/052F; National Center for Environmental Assessment Office of Research and Development U.S. Environmental Protection Agency: Washington, DC, USA, 2011.
53. US EPA. *Soil Screening Guidance: Technical Background Document*; Superfund US EPA: Washington, DC, USA, 1996.
54. MEPPRC. *Technical Guidelines for Risk Assessment of Contaminated Sites*; HJ25.3-2014; Ministry of Environmental Protection of the People's Republic of China: Beijing, China, 2014.
55. Li, Z.; Zhang, Y.; Wang, J.; Chen, C.; Zhang, Y.; Wang, P. A Survey on Dietary Types and Intake of Children Aged 3–12 in China. *China Food Nutr.* **2014**, *20*, 78–82.
56. He, Y.-N.; Zhao, L.Y.; Yu, D.-M. Vegetable and Fruit Intake Status of Adult Residents in China from 2010 to 2012. *Chin. J. Prev. Med.* **2016**, *50*, 221–224. [[CrossRef](#)]
57. US EPA. *Region IX, Regional Screening Levels (Formerly PRGs)*; US EPA: San Francisco, CA, USA, 2013.
58. Zhao, R.; Guan, Q.; Luo, H.; Lin, J.; Yang, L.; Wang, F.; Pan, N.; Yang, Y. Fuzzy Synthetic Evaluation and Health Risk Assessment Quantification of Heavy Metals in Zhangye Agricultural Soil from the Perspective of Sources. *Sci. Total Environ.* **2019**, *697*, 134126. [[CrossRef](#)]
59. Luo, H.; Wang, Q.; Guan, Q.; Ma, Y.; Ni, F.; Yang, E.; Zhang, J. Heavy Metal Pollution Levels, Source Apportionment and Risk Assessment in Dust Storms in Key Cities in Northwest China. *J. Hazard. Mater.* **2022**, *422*, 126878. [[CrossRef](#)] [[PubMed](#)]
60. Liu, Z.; Du, Q.; Guan, Q.; Luo, H.; Shan, Y.; Shao, W. A Monte Carlo Simulation-Based Health Risk Assessment of Heavy Metals in Soils of an Oasis Agricultural Region in Northwest China. *Sci. Total Environ.* **2023**, *857*, 159543. [[CrossRef](#)] [[PubMed](#)]
61. Wang, B.; Gao, F.; Qin, N.; Duan, X.; Li, Y.; Cao, S. A Comprehensive Analysis on Source-Distribution-Bioaccumulation-Exposure Risk of Metal(Loid)s in Various Vegetables in Peri-Urban Areas of Shenzhen, China. *Environ. Pollut.* **2022**, *293*, 118613. [[CrossRef](#)] [[PubMed](#)]
62. Tan, C. An Integrated Approach for Quantifying Source Apportionment and Source-Oriented Health Risk of Heavy Metals in Soils near an Old Industrial Area. *Environ. Pollut.* **2023**, *323*, 121271. [[CrossRef](#)]

**Disclaimer/Publisher's Note:** The statements, opinions and data contained in all publications are solely those of the individual author(s) and contributor(s) and not of MDPI and/or the editor(s). MDPI and/or the editor(s) disclaim responsibility for any injury to people or property resulting from any ideas, methods, instructions or products referred to in the content.